

RESEARCH ARTICLE

Ckmt1 is Dispensable for Mitochondrial Bioenergetics Within White/Beige Adipose Tissue

Valerie Politis-Barber¹, Heather L. Petrick¹, Arthe Raajendiran², Genevieve J. DesOrmeaux¹, Henvier S. Brunetta^{1,3}, Larissa M. dos Reis⁴, Marcelo A. Mori³, David C. Wright¹, Matthew J. Watt², Graham P. Holloway^{1,*}

¹ Department of Human Health and Nutritional Sciences, University of Guelph, 50 Stone Rd E, Guelph, ON N1G 2W1, Canada, ² Department of Anatomy and Physiology, The University of Melbourne, Parkville, VIC 3010, Australia, ³ Department of Biochemistry and Tissue Biology, University of Campinas, Campinas - SP 13083-970, Brazil and ⁴ Department of Genetics, Evolution, Microbiology and Immunology, University of Campinas, Campinas - SP 13083-970, Brazil

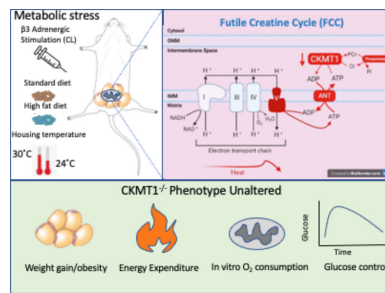
*Address correspondence to G.P.H. (e-mail: ghollowa@uoguelph.ca)

Abstract

Within brown adipose tissue (BAT), the brain isoform of creatine kinase (CKB) has been proposed to regulate the regeneration of ADP and phosphocreatine in a futile creatine cycle (FCC) that stimulates energy expenditure. However, the presence of FCC, and the specific creatine kinase isoforms regulating this theoretical model within white adipose tissue (WAT), remains to be fully elucidated. In the present study, creatine did not stimulate respiration in cultured adipocytes, isolated mitochondria or mouse permeabilized WAT. Additionally, while creatine kinase ubiquitous-type, mitochondrial (CKMT1) mRNA and protein were detected in human WAT, shRNA-mediated reductions in *Ckmt1* did not decrease submaximal respiration in cultured adipocytes, and ablation of CKMT1 in mice did not alter energy expenditure, mitochondrial responses to pharmacological β_3 -adrenergic activation (CL 316, 243) or exacerbate the detrimental metabolic effects of consuming a high-fat diet. Taken together, these findings solidify CKMT1 as dispensable in the regulation of energy expenditure, and unlike in BAT, they do not support the presence of FCC within WAT.

Submitted: 3 May 2022; Revised: 5 July 2022; Accepted: 7 July 2022

© The Author(s) 2022. Published by Oxford University Press on behalf of American Physiological Society. This is an Open Access article distributed under the terms of the Creative Commons Attribution-NonCommercial License (<https://creativecommons.org/licenses/by-nc/4.0/>), which permits non-commercial re-use, distribution, and reproduction in any medium, provided the original work is properly cited. For commercial re-use, please contact journals.permissions@oup.com



Key words: mitochondria; creatine; futile cycling; creatine kinase; adipose tissue; energy expenditure; browning; beiging; metabolism; mitochondrial bioenergetics

Introduction

Identifying mechanisms to decrease mitochondrial coupling has gained considerable interest as a therapeutic approach to promote energy expenditure and treat obesity. Within this context, brown adipose tissue (BAT) has been identified as a possible target tissue as a result of its highly specialized ability to dissipate chemical energy as heat through abundant expression of uncoupling protein 1 (UCP1).^{1–6} While BAT abundance is limited in humans,^{7,8} adipocytes within white adipose tissue (WAT) can develop a BAT-like phenotype in response to various stimuli,^{9–12} and this phenomenon, termed “browning” or “beiging” is characterized by the induction of multilocular adipocytes, robust mitochondrial biogenesis, increased expression of thermogenic genes (eg, *Ucp1*, *Cidea*, and *Pgc1 α*), and augmented mitochondrial respiration.^{13,14} Browning of WAT and the presence of functional beige adipocytes have been documented in the inguinal WAT of rodents and supraclavicular region of humans,^{15–18} and transplantation of these cells attenuated obesity and associated hyperglycemia in mice.¹⁹ Considering that in obese populations WAT depots can comprise up to 60%–70% of body mass,²⁰ promoting energy expenditure within WAT represents a promising and readily available “inducible” target in humans.

Independent of UCP1, creatine-dependent adenosine diphosphate (ADP) recycling in adipocytes has been proposed to stimulate energy expenditure.^{21,22} First described in beige adipocyte mitochondria, the creatine kinase mediated production of phosphocreatine (PCr) drives the liberation of a molar surplus of ADP to stimulate mitochondrial respiration in ADP-limited conditions.²¹ In this model, ADP is transported into the mitochondrial matrix through adenine-nucleotide transporter (ANT) to be utilized by adenosine triphosphate (ATP) synthase as a substrate for ATP production,²¹ while a phosphatase enzyme that is unidirectional regenerates creatine and inorganic phosphate at the expense of PCr. This continuous futile recycling of creatine (FCC) and ADP has been proposed to stimulate energy expenditure.^{21,22} In support of this model, preventing creatine transport by gene deletion of the creatine transporter, Solute Carrier Family 6 Member 8 (encoded by *Slc6a8*), or deleting the rate-limiting enzyme for creatine synthesis (glycine amidinotransferase, *GATM*), reduced creatine levels in adipocytes, and predisposed animals to obesity.^{23,24} Despite evidence in rodents suggesting that creatine is functionally involved in thermogenic pathways in adipose tissue, creatine monohydrate supplementation had no effect on BAT activation or energy expenditure in a human population known to have reduced creatine levels,²⁵ challenging the therapeutic potential of creatine-mediated energy expenditure within BAT.

The regeneration of PCr, regulated by creatine kinase, is critical for the proposed futile cycling of ADP. Four creatine kinase isoenzymes exist in mammals—historically two cytosolic forms ([creatine kinase, muscle-type (CKM)] and [creatine kinase, brain-type (CKB)]) and two mitochondrial forms ([creatine kinase ubiquitous-type, mitochondrial (CKMT1)], and [creatine kinase sarcomeric-type, mitochondrial (CKMT2)]), which exhibit differential tissue expression and are encoded by different genes,^{26,27} have been identified. Despite being classified as a cytosolic protein, a recent report has suggested that CKB is targeted to the mitochondria to regulate the FCC in brown adipocytes, and adipocyte-specific *CKB*^{-/-} mice have impaired energy expenditure and were susceptible to obesity.²⁸ However, it remains unclear if CKB is a key protein regulating mitochondrial bioenergetics within WAT, as within WAT CKB is not detected on mitochondrial membranes, and siRNA-mediated reductions in CKB only reduced cytosolic creatine kinase activity.²⁹ Additionally, reductions in CKB within WAT increases ADP-limited respiration and PCr concentrations,²⁹ responses opposite to the proposed CKB-mediated ADP recycling within the mitochondrial intermembrane space identified in BAT.²⁸ Apart from CKB, the mitochondrial isoforms CKMT1 and CKMT2 have been proposed to be important for energy expenditure as both proteins have been detected in human WAT²⁹ and BAT,^{30,31} and knockdown of *Ckmt1*²¹ and *Ckmt2*²⁹ in cultured human white adipocytes reduced basal mitochondrial respiration²¹ and mitochondrial creatine kinase activity.²⁹ Additionally, in mice consumption of a high-fat diet (HFD) increased *Ckmt1* and *Ckmt2* expression in visceral and subcutaneous WAT, respectively, suggesting possible adaptations to promote creatine-mediated energy expenditure with chronic energy overload within WAT.²⁴ As a result, in the present study, it was hypothesized that *Ckmt1* would represent a key creatine kinase mediating FCC within WAT. To interrogate this possibility, we evaluated the ability of creatine to support WAT mitochondrial respiration, determined which creatine-mediated proteins were expressed in human visceral adipose tissue, and given the presence of *Ckmt1*, determined if genetically decreasing *Ckmt1* affected mitochondrial bioenergetics, prevented β_3 -agonist mediated changes in energy expenditure, or exacerbated HFD-induced WAT hypertrophy and whole-body glucose intolerance in mice.

Methods

Animals

When explicitly stated, experiments utilized male Sprague Dawley rats that were bred on site at the University of Guelph.

Ckmt1 null (KO) and wild-type (WT) mice were bred on site at the University of Guelph from creatine kinase ubiquitous-type, mitochondrial (*CKMT1*; *Ckmt1^{tm2Bew}*) heterozygous mice. The colony was previously established from cryopreserved embryos, which were generously provided by Dr. Be Wieringa from Dr. Craig Lygate's repository and generated on a C57BL/6N background at the Toronto Centre for Phenogenomics, as previously described.³² All animals were group-housed in a temperature and humidity-regulated room on a 12:12-h light–dark cycle and were randomized to receive either (i) intraperitoneal (IP) injections of CL 316, 243 (CL; 0.2 mg/kg body mass; Sigma, C5976) or an equal volume of sterile saline (SAL) for 4 consecutive days ($n = 6$ –10/group), or (ii) sucrose matched low-fat control diet (LFD; 10% kcal from lard; Research Diets D12450) or (HFD; 60% kcal from lard; Research Diets D12492) for either 8 wk (animals housed at 24°C) or 5 wk (animals housed at 30°C). A shorter feeding intervention was selected for animals housed at thermoneutrality to increase the likelihood of detecting subtle differences in phenotype afforded by the ablation of *Ckmt1*. In all experiments, prior to tissue collection, an intraperitoneal injection of sodium pentobarbital (60 mg/kg; MTC Pharmaceuticals, Cambridge, ON, Canada) was used to anesthetize animals. All experiments were approved by the Animal Care Committee at the University of Guelph and met the guidelines of the Canadian Council on Animal Care.

Mitochondrial Isolation and Respiration

Mitochondria were isolated as previously reported with minor modifications. In brief, tissue was weighed [pooled WAT (iWAT and gWAT ~6 g) or red gastrocnemius (RG) (~200 mg)], minced with sharp scissors, and homogenized using a Teflon pestle (750 rpm). Thereafter, the homogenate was centrifuged (800 g; 10 min at 4°C), the supernatant centrifuged (9400 g; 10 min at 4°C), and, finally, mitochondria recovered by resuspending the pellet following a final spin (12 000 g; 10 min at 4°C). To remove excess lipid from WAT, homogenate was filtered with a cheese cloth prior to following the first centrifugation step. Permeabilized iWAT, gWAT, and muscle fibers (PMFs: red gastrocnemius) were prepared as previously described.^{32–38} For WAT experiments only MiR05 buffer was utilized. Mitochondrial respiration was detected using high-resolution respirometry (Oroboros Oxygraph-2 K, Innsbruck, Austria). Experiments were carried out at 37°C, with constant stirring (750 rpm), and concentrations of substrates are listed in figure legends. Respiration data were normalized to mitochondrial protein content or tissue weight.

Creatine Metabolism-Related Proteins in Human WAT

We have previously determined the transcriptome analysis of visceral WAT (VFAT) progenitor cells ($n = 5$) and adipocyte proteome in human upper-body subcutaneous WAT (ASAT), glutealfemoral WAT (GFAT), and VFAT.^{39,40} We utilized these data sets to determine the possible presence of proteins specifically linked to creatine metabolism.

shRNA of *Ckmt1*

The pLKO.1-puro lentiviral vector (Addgene #8453) was used to clone shRNAs contained the following target sequences: GFP (5'-CAAGCTGACCCTGAAGTTCAT-3'), *Ckmt1.a* (5'-GTGATCCAAGAGCGGCATAAT-3'), or *Ckmt1.b* (5'-GCCACTGCTGAGCAAAGATAA – 3'). Annealed oligos were cloned into AgeI-EcoRI restriction sites and viral particles packing was

performed in the HEK-293 cell line using psPAX2 (Addgene #12260) and pMD2.G (Addgene #12259) plasmids.

Murine white subcutaneous (9W) preadipocytes were cultured until confluence and differentiated with Dulbecco's modified Eagle's medium (DMEM; Sigma-Aldrich) containing 20 nM insulin, 1 nM triiodothyronine, 0.5 mM isobutyl methylxanthine, 1 μM dexamethasone, rosiglitazone 1 μg/mL, and 0.125 mM indomethacin according to the protocol published elsewhere.⁴¹ Differentiated 9W adipocytes were transduced with lentiviral particles (MOI 1) from the pLKO.puro shGFP or pLKO.puro *Ckmt1.a/b* on the last day of differentiation (day 8) for 24 h. Then, lentiviral particles were removed, and adipocytes were kept for another 3 d for oxygen consumption or gene expression measurements.

Seahorse Assay

Adipocytes (3×10^4) were seeded in a 24-well plate coated with gelatin 0.1% (Sigma-Aldrich) one day before the experiment and oxygen consumption rate (OCR) was measured with an XFe96 Seahorse Extracellular Flux Analyzer (Agilent) using a Cell Mito Stress Test kit. For measurements of basal OCR, cells were incubated in a medium supplemented with 1 mM pyruvate, 2 mM glutamine, and 10 mM glucose. Mitochondrial respiration was assessed by the addition (final concentration) of 0.01 mM creatine, 1 μM oligomycin, FCCP 1 μM (uncoupler), and 1 μM rotenone + antimycin A (complex I and complex III inhibitors, respectively). BCA protein assay was performed to estimate the protein concentration and normalize absolute OCR data.

qPCR

Gene expression analysis was performed by qPCR as previously described.⁴¹ In brief, RNA was extracted using TRizol (Thermo Scientific) and cDNA was synthesized using a High Capacity cDNA Reverse Transcription Kit (Applied Biosystems) following the manufacturer's instructions. qPCR was conducted using QuantiNova SYBR Green/ROX qPCR Master Mix (Qiagen). The primer sequences will be made available upon request. Gene expression was normalized by GAPDH.

Genotyping

Animal genotypes were confirmed with DNA extracted from mouse tail snips and WAT tissue using the AccuStart II PCR Genotyping Kit (Quantabio, #95135-500) according to the manufacturer's instructions using primers to detect wild-type (*Ckmt1^{+/+}*) and knockout (*Ckmt1^{-/-}*) alleles as follows: *Hyg1* 5'-GGCTGGCACTCTGTGATACCC-3'; *scCKmt1* 5'-TAGGCAGAAGGTATCTGCTGATGC-3'; *scCKmt28* 5'-CATGCCAACTACTACTGTTG TTCCT-3'.

Indirect Calorimetry

Mice were individually housed at 24°C in metabolic cages within the Oxymax Comprehensive Lab Animal Monitoring System (CLAMS; Columbus Instruments, Columbus, OH, USA). Diet and water were provided *ad libitum* and the same light–dark cycle was maintained. Total carbohydrate and fat oxidation and energy expenditure were calculated from VO₂ and VCO₂ as previously described.^{32,43}

Intraperitoneal Glucose and Insulin Tolerance Tests

Animals were fasted for 4 h prior to receiving an intraperitoneal injection of glucose (2 g/kg body mass) or insulin (1 U/kg body mass, Novorapid). Blood glucose was measured through the tail vein using a hand-held glucometer (Freestyle lite, Abbott Laboratories, Saint-Laurent, QC, Canada), and the area under the curve (AUC) was calculated by subtracting baseline blood glucose.

Histology

Histological assessment was carried out on iWAT, gWAT, and BAT samples that were fixed for 24 h in 10% neutral buffered formalin and transferred to 70% ethanol for storage at 4°C. Samples were embedded and stained on glass slides with hematoxylin and eosin (H&E) at the University of Guelph Animal Health Laboratory. Slides were imaged with Cell Sense software (Olympus, Tokyo, Japan) at 40x magnification to assess the adipocyte cross-sectional area (CSA) in iWAT and gWAT using an Olympus FSX 100 light microscope (Tokyo, Japan). The average of 4 fields per animal were captured and analyzed using the ImageJ software (National Institutes of Health) to quantify CSA.

Western Blotting

Tissue was homogenized, diluted to equal protein concentrations, separated by SDS-PAGE, transferred onto PVDF membranes, and detected using enhanced chemiluminescence substrate (ECL; Bio-Rad, #170-5061) on the FluorChem HD Imaging system (Alpha Innotech, Santa Clara, CA, USA). Commercially available primary antibodies were used to detect the creatine kinase ubiquitous-type, mitochondrial (CKMT1; 1:5000, ab131188; Abcam), creatine kinase, brain-type (CKB; 1:1000, A12631; Abclonal), complexes of the electron transport chain (OXPHOS; 1:500, ab110413; Abcam), peroxisome proliferator-activated receptor gamma coactivator 1 α (PGC1 α ; 1:1000, #516557; Calbiochem), UCP1, 1:2000, ab10983; Abcam), and cytochrome c oxidase subunit IV (COXIV; 1:10 000, A21347; Invitrogen). All samples within a set were loaded onto 1 membrane to limit variation, and equal loading was confirmed with Ponceau staining, where appropriate.

Statistical Assessment

All statistical analyses were carried out using Prism 9 (Graph Pad Software, Inc., La Jolla, CA, USA). The apparent K_m for ADP was determined via Michaelis–Menten kinetics and is defined as the concentration of ADP, which achieves half maximal mitochondrial respiration (V_{max}). Unpaired t-tests were utilized to compare the apparent K_m and $\% \Delta K_m$ with creatine from ADP titrations in RG, adjusted by Benjamini–Hochberg FDR. All other data were compared using either a one-way (human data) or a two-way ANOVAs, followed by Fisher LSD *post-hoc* analyses where appropriate. Data are expressed as mean \pm standard error of the mean (SEM), and the statistical significance was set at $P < .05$.

Results

Assessing the FCC

As creatine cycling has been suggested to promote ADP recycling in mitochondria isolated from iWAT in diverse situations,^{21,23,24} we first investigated the stimulatory effect of creatine on *in vitro* mitochondrial bioenergetics. To achieve this, we adapted a

well-established technique for isolating mitochondria in skeletal muscle (Figure 1A).^{32,44,45} Due to the relatively high WAT requirement, rats were utilized to eliminate the need to pool multiple mice for a single mitochondrial isolation. The P/O ratios from isolated WAT mitochondria were comparable to skeletal muscle RG and values reported in the literature,^{46,47} validating our experimental model (Figure 1A). Next, we examined whether the addition of creatine would increase submaximal ADP-supported respiration and/or decrease P/O ratios within WAT, both indicative of creatine-driven recycling of ADP. Creatine had no significant effects on submaximal ADP respiration, maximal complex I/II respiration, or P/O ratios in mitochondria isolated from WAT (Figure 1B inset and 1C). While these data suggest creatine does not increase oxygen utilization or promote recycling within WAT mitochondria, for the proposed FCC model to be functional, creatine kinase would need to be retained in the intermembrane space (Figure 1D). While CKMT1 was detectable in isolated mitochondria (Figure 1C inset), it was not concentrated like other mitochondrial proteins (Figure 1C inset), possibly limiting the *in vitro* stimulatory effects of creatine. We therefore tested the ability of creatine to stimulate respiration in permeabilized WAT, a model that would contain all endogenously expressed creatine-related proteins. Since the original experiments detecting FCC were performed in mice,^{21,22} we also wanted to ensure species differences were not confounding our interpretation. Similar to rat isolated mitochondria (Figure 1B and C), creatine did not stimulate submaximal ADP-supported respiration in either inguinal or gonadal WAT from mice (iWAT, gWAT) (Figure 1E and F), but creatine did stimulate submaximal respiration in permeabilized skeletal muscle fibres (Supplementary Figure S1). While these experiments suggest creatine does not stimulate ADP recycling in unstimulated WAT, the original experiments were conducted following cold exposure and CL 316,243 (CL) administration in mice,^{21,22} raising the possibility that β_3 -adrenergic mediated gene transcription could be required for the detection of FCC. We therefore assessed the possible creatine-mediated futile cycling in WAT from mice after CL stimulation. CL administration increased the abundance of OXPHOS proteins and UCP1 in isolated mitochondria, responses indicative of β_3 -adrenergic mediated being (Figure 1G inset). In contrast to unstimulated tissue (Figure 1B), presumably as a result of increased UCP1 (Figure 1G inset), P/O ratios following CL administration could not be determined because of an apparent uncoupling (Figure 1G). As a result, we determined the total oxygen utilization over 5 min in the presence and absence of creatine. Even with this approach creatine did not result in greater oxygen utilization when stimulated with submaximal ADP concentrations (Figure 1H), suggesting β_3 -adrenergic signaling does not induce FCC in WAT. While we could not detect creatine-stimulated ADP recycling in isolated mitochondria following CL administration (Figure 1H), the increased content of UCP1 may have prevented the detection of creatine-mediated ADP recycling (Figure 1I). It is difficult to model the *in vivo* activity of UCP1 in an *in vitro* isolated mitochondrial preparation, as the biological concentration of purine nucleotides guanosine diphosphate ([GDP] and ADP) and inorganic phosphate are all removed in this preparation.⁴⁸ Additionally, isolated mitochondria do not retain their native architecture/size,⁴⁹ and swelling of mitochondria may impact membrane fluidity and rates of fatty acid flip flop (considered rate-limiting for H⁺-mediated uncoupling at a neutral pH), or increase the pH of the intermembrane space (ie, increased volume to dilute H⁺), which places a larger emphasis on direct H⁺ transport by UCP1.^{50,51} Given these methodological considerations we utilized a permeabilized

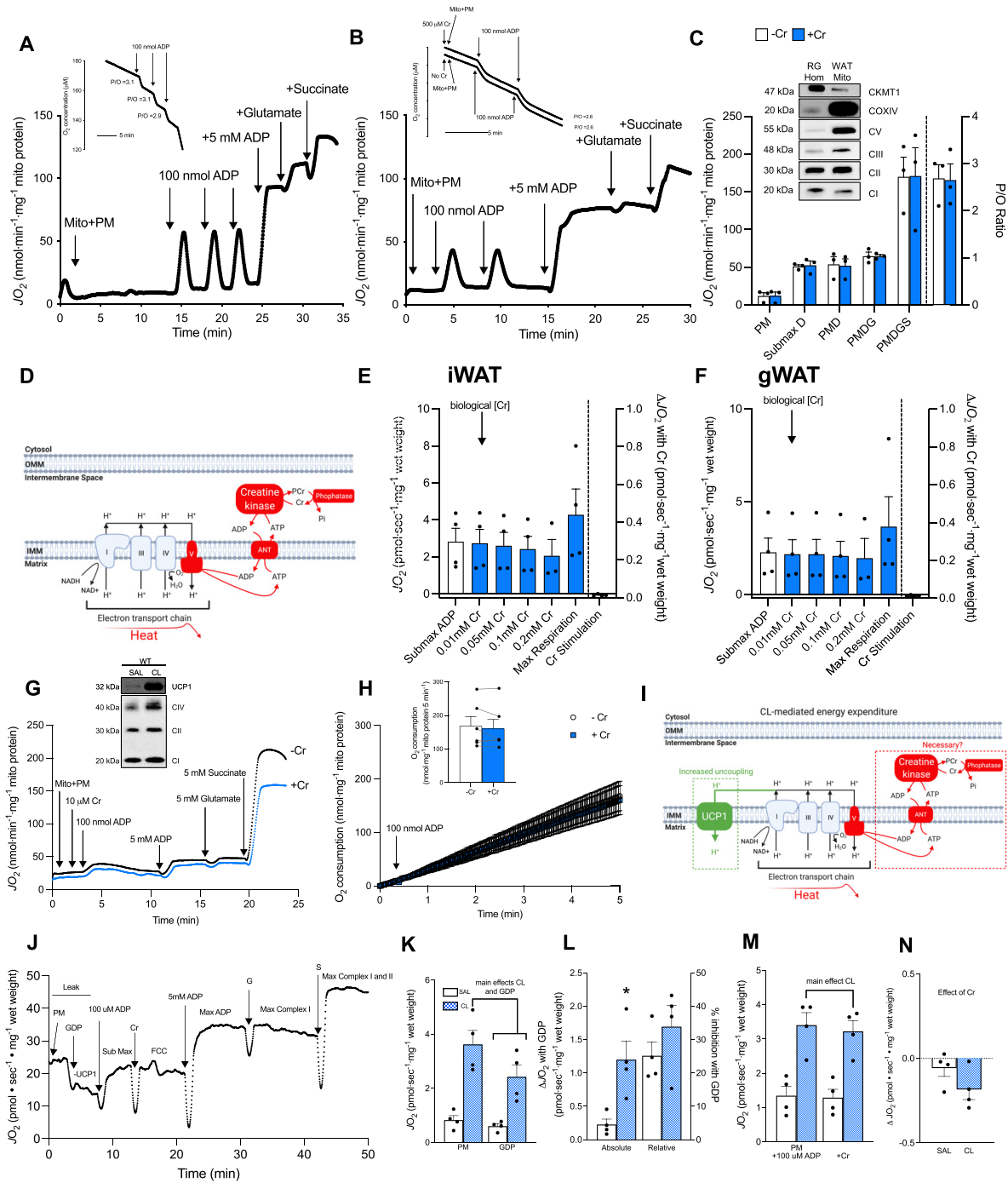


Figure 1. Creatine does not stimulate mitochondrial respiration in isolated white adipose tissue mitochondria with or without β -adrenergic stimulation with CL 316,243. Representative traces of isolated RG as a positive control (A), and white adipose tissue [WAT, (B)] mitochondria from rats, whereby the addition of creatine in WAT did not alter submaximal or maximal complex I/II respiration or P/O ratios (C), and representative images of western blots comparing protein content from RG homogenate and isolated mitochondria from WAT (inset of C). Schematic depicting the proposed futile creatine cycle (FCC) in the mitochondria (D), and creatine titrations in the presence of submaximal ADP in iWAT (E) and gWAT (F). Representative trace of respiration in the presence and absence of creatine in isolated mitochondria from WAT of mice following β -adrenergic induced signaling depicting an inability to determine coupling ratios (G) or a creatine-mediated stimulation in oxygen consumption. Representative western blots in isolated mitochondria following saline (SAL) or CL 316,243 (CL) injections showing the upregulation of (UCP1: G inset). Real-time respiratory trace depicting oxygen utilization over 5 min in the presence of submaximal ADP following CL administration (H: inset is total oxygen use over 5 min). Schematic depicting CL-induced UCP1 and absence of a requirement for FCC-mediated ADP recycling for electron transport chain flux (I). Real-time respiratory trace depicting oxygen utilization over 5 min in the presence of submaximal ADP following CL administration (J). Quantified leak respiration in the presence and absence of GDP (K), GDP-mediated inhibition (L), respiration in the presence and absence of creatine (M), and the ability of creatine to stimulate respiration (N) in iWAT following CL administration. ANT, adenine nucleotide transporter; CI-V complexes I-V of the electron transport chain; CKMT1, creatine kinase ubiquitous-type, mitochondrial; COXIV, cytochrome c oxidase subunit IV; Cr, creatine; GDP, guanosine diphosphate; IMM, inner mitochondrial membrane; NAD, nicotinamide dinucleotide; OMM, outer mitochondrial membrane; PM, pyruvate + malate; PMD, PM + ADP; PMDG, PM + glutamate; PMDGS, PMD + succinate; UCP1, uncoupling protein-1. Data expressed as mean \pm SEM. * is different ($P < .05$) from saline.

tissue approach to assess mitochondrial respiration following CL (Figure 1J). CL markedly increased leak respiration (Figure 1K) and oxidative phosphorylation (Supplementary Figure S2) ~5-fold in iWAT. Guanosine diphosphate attenuated respiration to a greater extent following CL (Figure 1L), which presumably resulted from increased UCP1 content. However, the relative inhibition exerted by GDP was similar following CL (Figure 1L), suggesting that unlike isolated mitochondria, H⁺ conductance was retained in this *in vitro* model following CL administration. Importantly, in the presence of GDP-mediated inhibition of UCP1, creatine did not stimulate submaximal ADP stimulated respiration following CL (Figure 1M and N). The present data highlight β_3 -adrenergic signaling as an inducer of uncoupled/nonoxidative phosphorylation dependent respiration through the induction of UCP1, and challenges the necessity of ADP recycling for energy expenditure when being occurs.

Determining the Expression of Creatine-linked Genes in Human WAT

While we could not detect creatine-stimulated ADP recycling in either isolated mitochondria or in permeabilized WAT, it remains possible that the FCC is biologically relevant for energy expenditure. We therefore examined existing mRNA data that we previously published in human WAT progenitor cells separated based on the abundance of CD34 protein (Figure 2A).³⁹ We utilized this methodology as human WAT progenitor cells with abundant CD34 (CD34^{hi}) are linked with greater cross-sectional area and triglyceride esterification, while the absence of CD34 (CD34⁻) is associated with beige characteristics, including higher expression of PPARGC1A (which encodes PGC1 α) and UCP1.³⁹ We therefore hypothesized that FCC related genes would be more abundantly expressed in CD34⁻ progenitor cells. In the present study, while we detected genes involved in creatine synthesis (SLC6A8, GATM and GAMT: Figure 2B) and creatine kinase (CKMT1, CKMT2 and CKM: Figure 2C), these genes were all detectable in both CD34⁻ and CD34^{hi} progenitor cells (Figure 2C). We also detected three alkaline phosphatases (CNTAP1, CNTNAP2 and ALPL; Figure 2D), although none was abundantly expressed in CD34⁻ progenitor cells. Since CD34⁻ cells have been linked to beige/energy dissipating characteristics,³⁹ and in general CD34⁻ cells express an abundance of genes encoding creatine-mediated proteins (Figure 2B and C), we re-examined our previously published proteomic data to determine the possible abundance of proteins involved in creatine metabolism (Figure 2E). While we identified 4220 proteins in human WAT, proteins involved in creatine metabolism, including SLC6A8, GATM, and GAMT, and possible alkaline phosphatases such as CNTNAP were not reliably detected (Figure 2F). In contrast, the alkaline phosphatase ALPL was detected in all WAT samples, and of the possible creatine kinase isoforms, only CKMT1 and CKB were detected in all samples (Figure 2F). However, the abundance of ALPL and the creatine kinase proteins displayed divergent hierarchical patterns, as while ALPL was less abundant in VAT, both CK proteins were most abundant in visceral WAT compared with subcutaneous WAT (Figure 2F). Altogether, while human WAT expresses several key creatine-related proteins, there appears to be an absence of coordination in these genes, limiting the possibility of creatine futile cycling, as alkaline phosphatases are preferentially expressed in progenitor cells associated with TAG storage (CD34^{hi}) and in subcutaneous WAT depots, while CK genes were conversely expressed in progenitor cells associated with beige phenotype

(CD34⁻) and in VAT. CKMT1 was the only CK isoform detected in both CD34⁻ progenitor cells transcriptome and in human WAT proteome.

CKMT1 Does Not Influence Fuel Utilization and Energy Expenditure During Acute β_3 -Adrenergic Stimulation with CL 316, 243

Since both mRNA and proteomic approaches demonstrate CKMT1 expression in human WAT, we next aimed to determine if CKMT1 directly regulates mitochondrial bioenergetics. In contrast to our hypothesis, in differentiated 9W white adipocytes, shRNA-mediated reductions (~80%) in *Ckmt1* (Figure 3A) increased submaximal respiration (Figure 3B and C, main effect), while the provision of creatine did not stimulate submaximal respiration in either control (GFP) or *Ckmt1* knock-down cells (Figure 3B and D). We next tested the possibility that ablating *Ckmt1* affected the biological response to various cellular stresses. To achieve this, we utilized a whole-body CKMT1 knockout (KO) mouse. Genotyping confirmed the absence of exon 3, which has been shown to render CKMT1 inactive,⁵² within WAT depots in KO animals (Figure 3E). Additionally, the ability of creatine to stimulate submaximal respiration was attenuated in the skeletal muscle of KO mice further verifying the absence of CKMT1³² (Supplementary Figure S1A and B). We next determined the role of CKMT1 in mediating β_3 -adrenergic induced energy expenditure. The acute induction of adaptive nonshivering thermogenesis through the administration of β_3 -adrenergic agonist CL increased VO₂, VCO₂, fatty acid oxidation, energy expenditure, and heat production, and decreased carbohydrate oxidation and respiratory exchange ratio (RER) (Figure 3F–M). Ablation of *Ckmt1* did not affect any of these metabolic parameters, suggesting CKMT1 does not influence whole-body energy expenditure with β_3 -adrenergic stimulation. Whole-body energy expenditure may not adequately reflect WAT metabolism; therefore we next assessed the influence of CKMT1 on WAT browning following 4 d of CL administration. CL decreased adipocyte cross-sectional area (gonadal WAT only), increased the number of multilocular lipid droplets (both inguinal WAT and gonadal WAT), and increased mitochondrial proteins in WT mice, morphological and molecular changes that are indicative of a beige-like phenotype (Figure 3N–W). However, the absence of CKMT1 did not affect these responses. Additionally, CKB content was not inducible with CL treatment in either iWAT or gWAT (Figure 3Q, R, V, and W). In support of these findings, distinct structural changes within interscapular BAT were observed following CL treatment, characterized by a striking visual reduction in lipid droplet size, which was not affected by genotype (Supplementary Figure S3). Hence, while CL administration had prominent effects on adipose tissue, overall, our data demonstrate that *Ckmt1* ablation does not influence CL-induced browning within iWAT and gWAT depots.

We next aimed to functionally assess the possibility that increasing CKMT1 protein through being with CL 316243 could affect *in vitro* respiration using a permeabilized tissue approach. While CL markedly increased respiration ~5-fold in both iWAT and gWAT regardless of genotype (main effect CL: Figure 4A and B), ADP was capable of stimulating respiration similarly following CL administration (Figure 4A and B). As a result, CL did not reduce the respiratory control ratio (respiration presence/absence of ADP: data not shown), further suggesting retained mitochondrial coupling in a permeabilized tissue

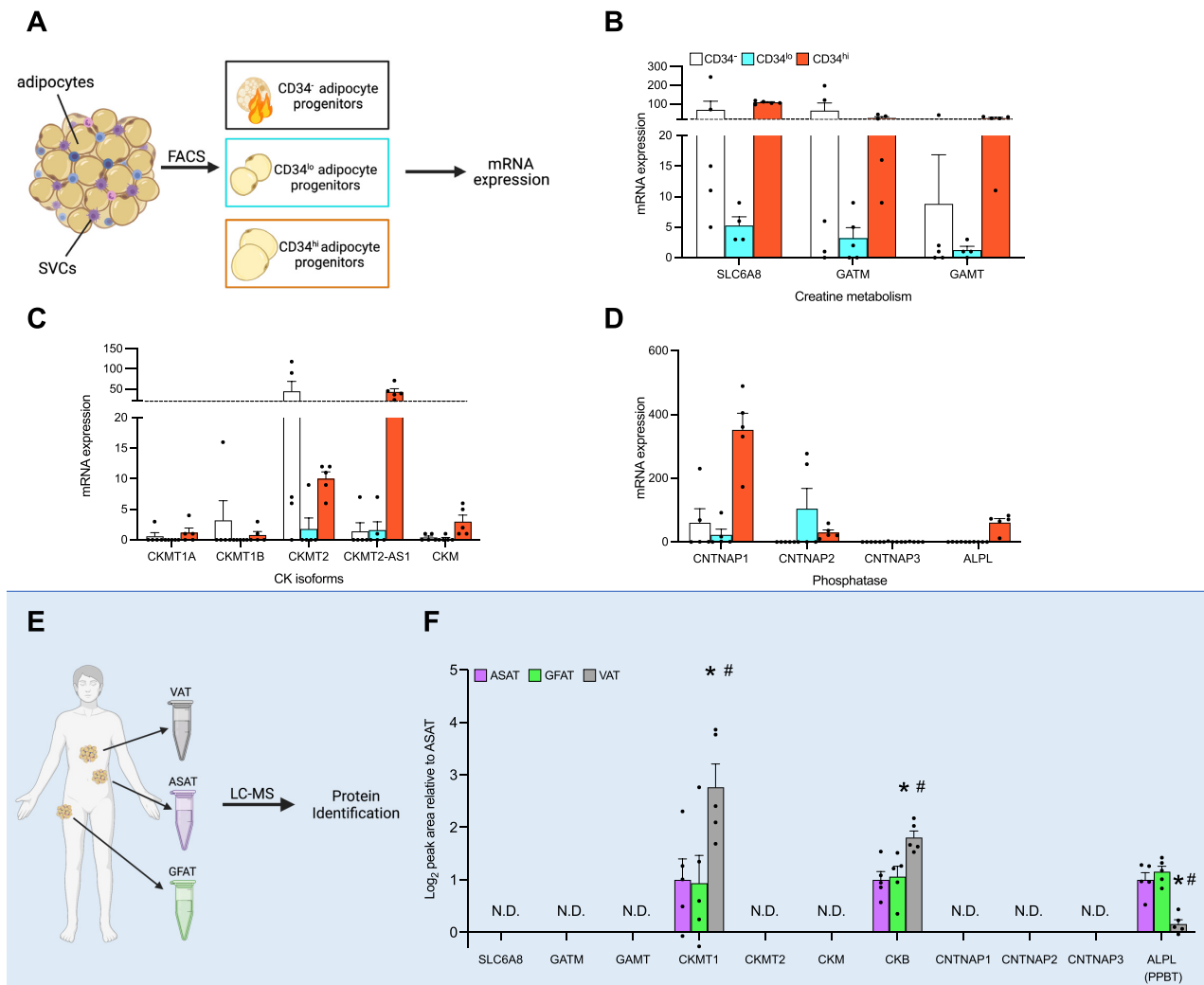


Figure 2. Detection of creatine kinase ubiquitous-type, mitochondrial (CKMT1) mRNA expression, and protein in human WAT. Visceral WAT (VAT) progenitor cells ($n = 5$) were separated based on the abundance of CD34 and used to determine the expression of genes (A) related to creatine metabolism (B), creatine kinase isoforms (C), and alkaline phosphatases (D). Human VAT, subcutaneous WAT (ASAT), and glutealfemoral WAT (GFAT) were also utilized to examine the content of creatine-related proteins (E), however only CKMT1, creatine kinase B (CKB) and ALPL could be detected (F). Creatine transport (Slc6a8), creatine synthesis [glycine amidinotransferase (GATM) and Guanidinoacetate methyltransferase (GAMT)]. Not detected (N.D.). Data expressed as mean \pm SEM. * is different ($P < .05$) from VFAT, and # is different from GFAT.

preparation, despite the increase in UCP1 protein (Figure 3). Nevertheless, under conditions of submaximal ADP, creatine failed to drive respiration in either depot, and in fact decreased respiration in the presence of creatine in iWAT (Figure 4C and D, inset is change with creatine). ADP sensitivity was unchanged by CL in iWAT (Figure 4E), while treatment in gWAT increased the apparent ADP K_m , indicative of a decrease in ADP sensitivity (Figure 4F). In both depots, genotype (Figure 4E and F) and creatine (data not shown) had no effect on ADP sensitivity. Combined, these functional data indicate that CL robustly increased mitochondrial respiration within iWAT and gWAT, and these responses were not altered by creatine or ablation of *Ckmt1*.

Ablation of *Ckmt1* Does Not Exacerbate HFD-Induced Glucose Intolerance and Weight Gain, or Alter Resting Metabolism

Given the proposed implication of CKMT1 in energy expenditure and the previous observation that HFD increased *Ckmt1* gene

expression within WAT,²⁴ we subsequently examined the possible contribution of CKMT1 to HFD-induced obesity and insulin resistance. In female mice, HFD feeding predictably induced glucose intolerance (Figure 5A and B), increased body mass (~ 10 g, Figure 5C), weekly caloric intake ($\sim 40\%$, Figure 5D), rates of fatty acid oxidation, and absolute energy expenditure during the dark cycle (Figure 5E–J). The increase in energy expenditure following HFD was not attributable to changes in movement activity (Figure 5K) and was mitigated when normalized to body weight, suggesting the absence of changes in bioenergetics (Figure 5L). High-fat diet also increased the cross-sectional area of adipocytes (Figure 6A–E), but ablating *Ckmt1* did not alter any of these morphological or functional responses, suggesting *Ckmt1* does not influence the phenotypic response to HFD consumption. Moreover, HFD feeding decreased submaximal ADP-supported respiration, maximal complex I/II-supported respiration (Figure 6F and I), and the apparent K_m for ADP (Figure 6H and K) in wildtype mice and ablating *Ckmt1* had no effects on mitochondrial respiration that were distinguishable from wildtype

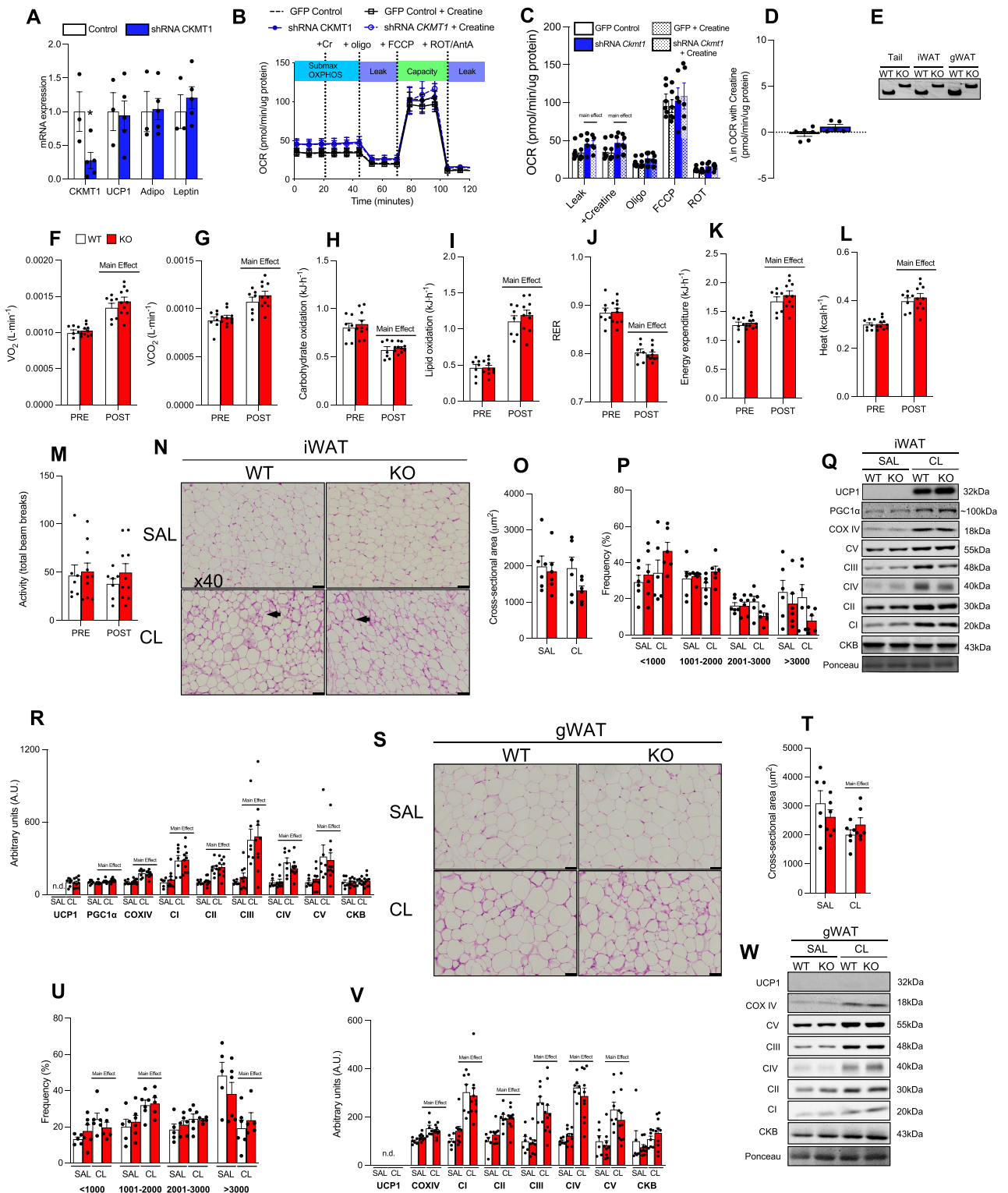


Figure 3. Decreasing *Ckmt1* in adipocytes (shRNA) and in mice (KO) does not affect mitochondrial bioenergetics. mRNA expression following shRNA of *Ckmt1* (A), adipocyte respiration in control (GFP), and shRNA-mediated *Ckmt1* knockdown cells in the presence and absence of creatine (B, C) and the creatine-mediated stimulation of respiration (D). Representative images of *Ckmt1* WT and KO genotyping (E) in various tissues. VO_2 (F), VCO_2 (G), carbohydrate oxidation (H), lipid oxidation (I), RER (J), energy expenditure (K), heat production (L), and activity (M) in WT and KO animals 3 h pre- and post- CL 316243 (0.2 mg \cdot kg $^{-1}$) injection. Representative images of stained with H&E from SAL and CL-treated mice imaged at x40 magnification (iWAT M, gWAT R), cross-sectional adipocyte area (iWAT N, gWAT S), frequency distribution of adipocytes by cross-sectional area (iWAT O, gWAT T), western blot analysis showing relative mitochondrial protein content, and representative images (iWAT P and Q, gWAT U and V) from male *Ckmt1* WT and KO animals. Arrows indicate the presence of multilocular lipid droplets and scale bars are 43 μ m. VO_2 , rate of oxygen consumption; VCO_2 , rate of carbon dioxide production; RER, respiratory exchange ratio. Ponceau staining was used as a loading control. Data expressed as mean \pm SEM.

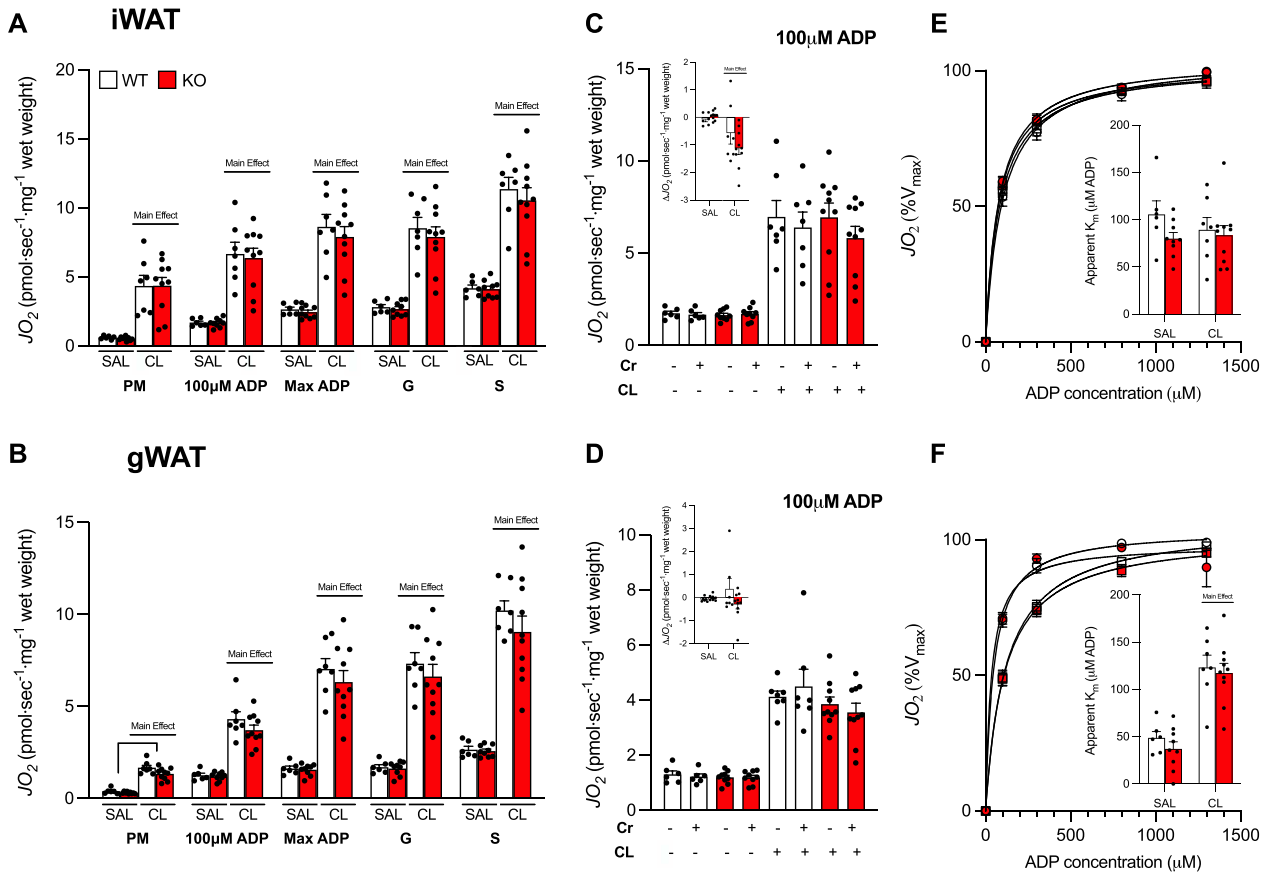


Figure 4. CL 316,243 treatment increases mitochondrial respiration similarly between *Ckmt1* WT and KO animals in iWAT and gWAT, and creatine does not enhance this change. Submaximal ADP and maximal complex I/II-supported respiration in iWAT (top, A) and gWAT (bottom, B), difference in submaximal ADP-supported respiration (C and D), and ADP respiratory kinetics with the calculated apparent K_m (E and F) in the presence and absence of creatine in male *Ckmt1* WT and KO animals. PM, pyruvate + malate; PMD, PM + ADP; PMDG, PM + glutamate; PMDGS, PMDG + succinate. Data expressed as mean \pm SEM.

mice. Notably, like our original experiments (Figure 1E and F), creatine did not drive mitochondrial respiration in the presence of submaximal ADP in either group or WAT depot (Figure 6G, H, J, and K). While these data indicate that the ablation of *Ckmt1* does not affect the susceptibility to HFD-mediated glucose intolerance, given the protection females are afforded against HFD-induced obesity,^{53,54} we wanted to confirm that our findings could be translated across the sexes by repeating metabolic experimental protocols in male mice. Aligning with our data in female mice, ablating *Ckmt1* did not alter HFD-induced glucose intolerance or indices of whole-body metabolism and energy expenditure (Supplementary Figure S4A–I). Combined, these data demonstrate that, regardless of sex, ablation of *Ckmt1* does not exacerbate mitochondrial dysfunction or changes in whole-body energy homeostasis in mice fed an HFD.

At Thermoneutrality, CKMT1 does not Influence HFD-Induced Glucose Intolerance, Insulin Resistance, or iWAT and gWAT Respiration

Given the previous findings suggesting the presence of FCC in WAT^{21,23,24} and our failure to detect FCC in mice, we were concerned that our housing of mice at thermoneutrality was masking the presence of FCC. While housing mice at ambient temperatures below their thermoneutral zone is widely common practice, it has been shown to mask the obesogenic effects of

HFD in UCP1 KO mice.⁵⁵ We reasoned that in a similar manner, housing temperature may be contributing to metabolic uniformity observed between *Ckmt1* WT and KO animals housed at room temperature. We therefore conducted additional experiments where mice were fed an HFD and housed at 30°C. Housing temperature did not alter the biological response to an HFD, as at thermoneutrality, regardless of genotype HFD-fed animals became glucose intolerant (Figure 7A and B) and insulin resistant (Figure 7C and D). Additionally, in permeabilized iWAT and gWAT, HFD consumption reduced mitochondrial respiration (Figure 7E and H) and the apparent K_m of ADP (Figure 7G and J) similarly in WT and *Ckmt1* KO mice (main effect of HFD). Moreover, in the presence of submaximal ADP, stimulation of respiration could not be detected with the addition of creatine in either genotype (Figure 7F and I). These data demonstrate that ablation of *Ckmt1* does not accelerate the progression of diet-induced obesity, even in mice housed at thermoneutrality.

Discussion

We aimed to determine the presence of creatine-mediated respiration in WAT in response diverse metabolic stimuli, and to establish the necessity of CKMT1 as a candidate enzyme regulating the FCC within WAT. However, despite the incorporation of various *in vitro* models (ie, differentiated adipocytes, isolated mitochondria, and permeabilized tissue) and cellular stress (ie, β_3 -adrenergic signaling, HFD, sex, and housing temperature), in

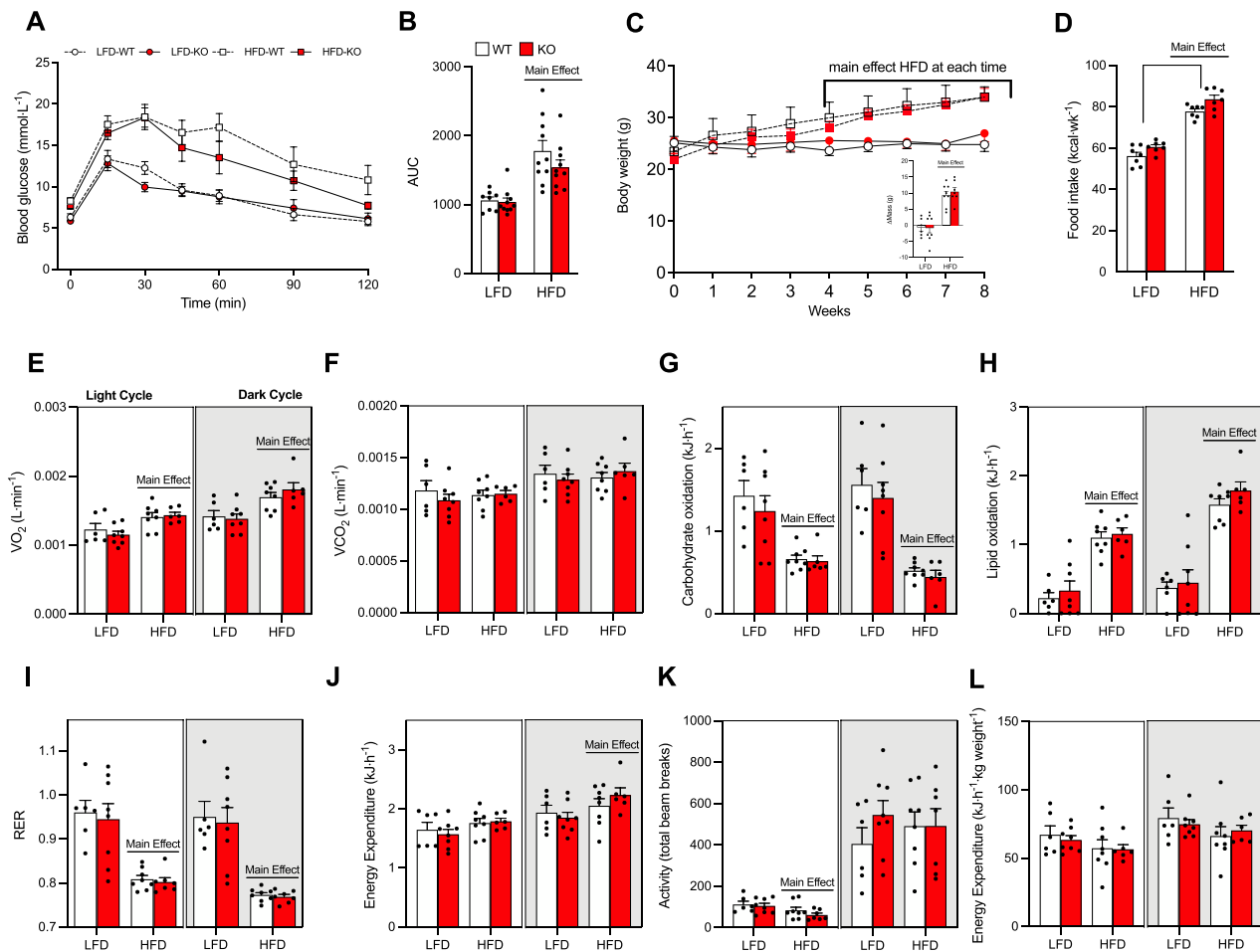


Figure 5. High-fat diet induced changes in glucose tolerance, weight gain, and resting whole-body metabolism are consistent between *Ckmt1* WT and KO mice. Glucose tolerance test (A), area under the curve (B), body mass (C: inset change in body mass), weekly food intake (D), VO_2 (E), VCO_2 (F), carbohydrate oxidation (G), lipid oxidation (H), RER (I), energy expenditure (J), activity (K), and energy expenditure normalized to body weight (L) in female *Ckmt1* WT and KO mice after 8 wk of LFD or HFD-feeding. AUC, area under the curve; VO_2 , rate of oxygen consumption; VCO_2 , rate of carbon dioxide production; RER, respiratory exchange ratio. Data expressed as mean \pm SEM.

contrast to our hypothesis we could not verify the presence of creatine-mediated substrate cycling as a primary determinant of mitochondrial respiration within WAT. Additionally, molecular approaches that reduced *Ckmt1* in cultured adipocytes and mice did not impair mitochondrial bioenergetics, solidifying *Ckmt1* as dispensable for regulating energy expenditure within WAT.

While it was hypothesized that CKMT1 was an important regulator of the FCC within WAT, ablating *Ckmt1* did not affect body weight, energy expenditure, glucose tolerance, or insulin sensitivity in HFD-fed animals, and neither sex nor housing temperature altered these responses. Furthermore, adipocyte hypertrophy and both basal and maximal respiration in iWAT and gWAT followed the anticipated changes in response to an HFD feeding, however, these indices were unaffected by genotype. These findings are in contrast to other gene deletion models (eg, UCP1, TNAP, CrT, and CKB), which exhibit pathological changes of metabolic parameters associated with obesity and insulin resistance^{23,28,55,56} suggesting CKMT1 is not a primary contributor to creatine-driven nonshivering thermogenesis as it pertains to obesity. While creatine has previously been reported to stimulate respiration within mitochondria isolated from BAT and beige/WAT,^{21,23,24,28,56} we could not verify this response in

mitochondria isolated from either rats or mice, as creatine did not impact P/O ratios or submaximal respiration. The physiological intervention used to induce beige adipose tissue could be a contributing factor in the discrepant findings, as while others have primarily used cold exposure²¹ to beige WAT, we employed pharmacological β_3 -AR activation with CL 316, 243. A recent report indicates cold and β_3 -ARs activate distinct populations of beige adipocytes within WAT^{57,58} and a preprint report shows cold-exposure stimulates FCC-linked genes to a greater degree than CL administration.⁵⁹ However, while the magnitude of the response may be different between CL and cold exposure, it is thought that browning of WAT through cold exposure is mediated primarily by β_3 -ARs^{60,61} and creatine has been shown to stimulate respiration in isolated mitochondria derived from WAT after CL administration in younger mice.^{21,22} Also, in the present study, CL was effective at eliciting canonical characteristics of adipocyte browning, including multicolority of lipid droplets, a marked increase in UCP1 (within iWAT) and markers of mitochondrial biogenesis, and respiratory capacity within several WAT depots. Alternatively, a difference between the present methodology and previous reports is the age of the mice, as young animals (5–7 wk of age) were utilized in previous experiments delineating creatine-mediated futile cycling²¹

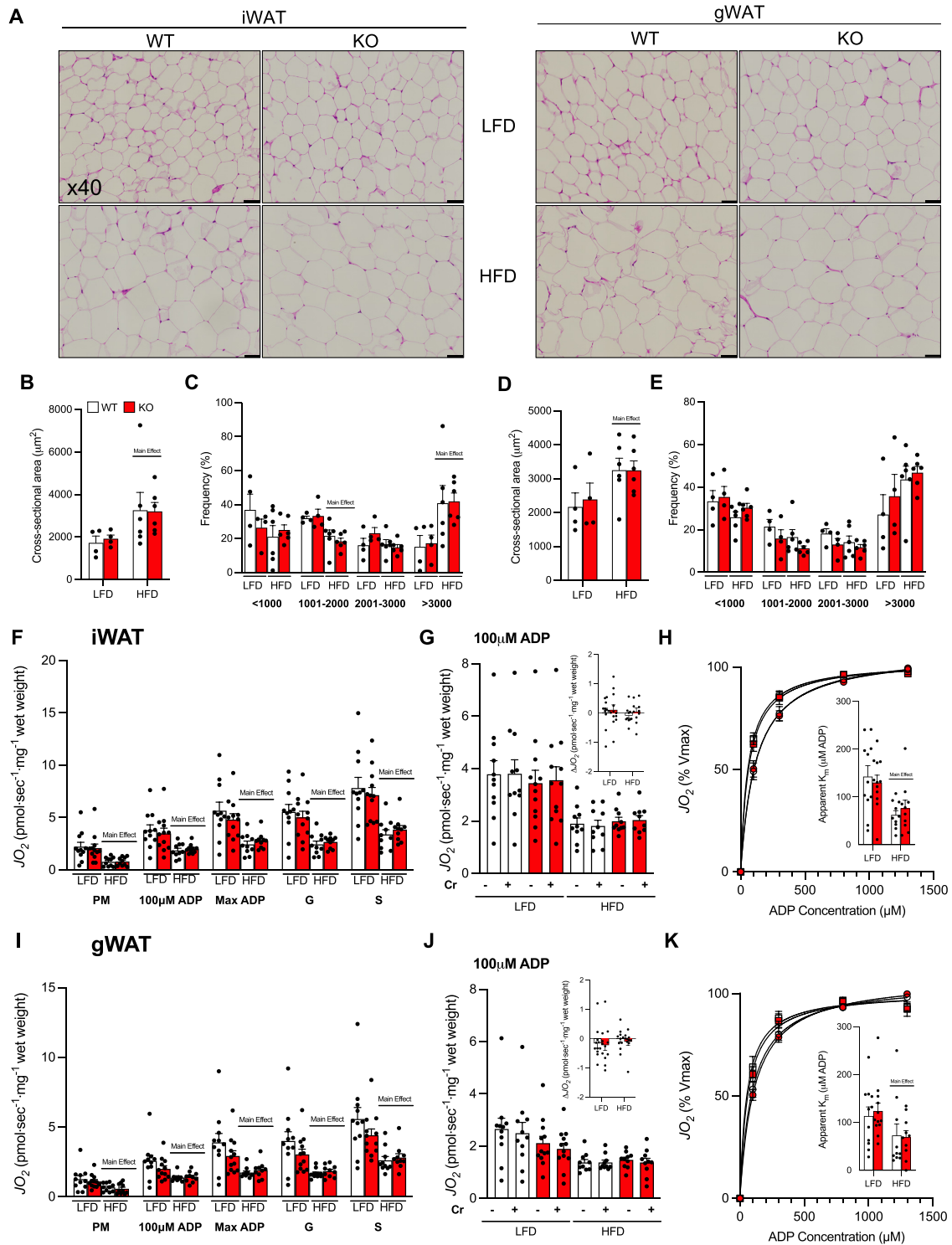


Figure 6. High-fat diet-induced adipocyte hypertrophy and reductions in mitochondrial respiration are consistent between *Ckmt1* KO and WT mice in iWAT and gWAT depots. Representative images of iWAT (left) and gWAT (right) stained with hematoxylin-and-eosin (H&E) imaged at x40 magnification (A), cross-sectional adipocyte area (B and D), and frequency distribution of adipocytes by cross-sectional area (C and E), from female *Ckmt1* WT and KO animals fed LFD or HFD for 8 wk. Additionally, submaximal ADP and maximal complex I/II-supported respiration in iWAT (top, F), and gWAT (bottom, I), difference in submaximal ADP-supported respiration (G and J), and ADP respiratory kinetics with the calculated apparent K_m (H and K) in the presence and absence of creatine. PM, pyruvate + malate; PMD, PM + ADP; PMDG, PM + glutamate; PMDGS, PMDG + succinate. Scale bars are 43 μM . Data expressed as mean \pm SEM

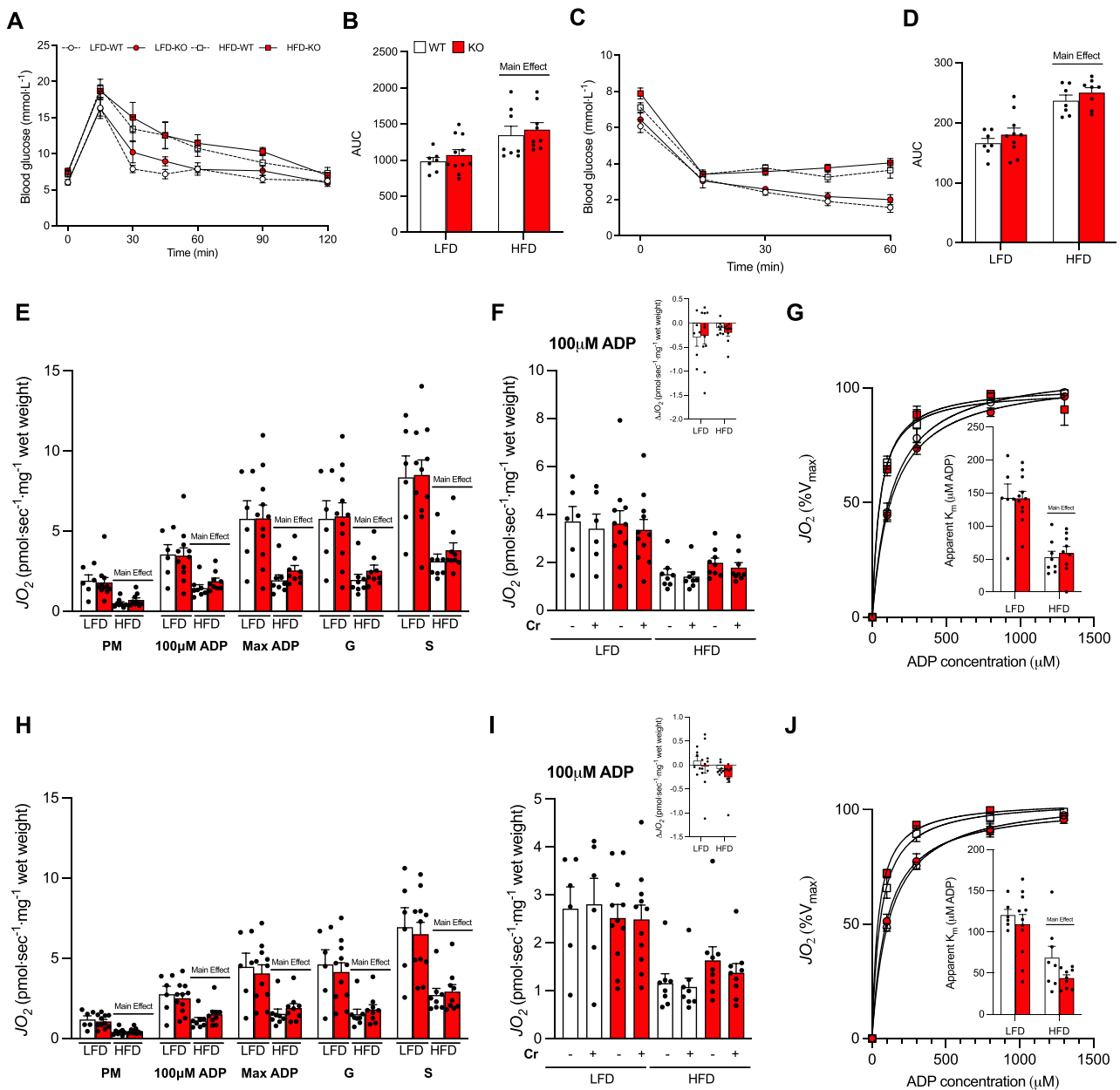


Figure 7. At thermoneutrality, *Ckmt1* KO animals display similar glucose tolerance, insulin sensitivity, and mitochondrial function on HFD compared to WT animals. GTT (A), glucose AUC (B), ITT (C), insulin AUC (D), submaximal ADP and maximal complex I/II-supported respiration in iWAT (top, E), and gWAT (bottom, H), difference in submaximal ADP-supported respiration (F and I), and ADP respiratory kinetics with the calculated apparent K_m (G and J) in the presence and absence of creatine in female *Ckmt1* WT and KO mice after 5 wk of LFD or HFD-feeding. PM, pyruvate + malate; PMD, PM + ADP; PMDG, PM + glutamate; PMDGS, PMDG + succinate. Data expressed as mean \pm SEM.

compared with older mice (18–24 wk) in the present study. Since adipose tissue browning regresses with ageing,⁶² this may have contributed to the inability to detect an effect of creatine in the present study. However, if this point is accurate this raises questions about the translatability of the FCC to adult humans, especially since creatine supplementation does not affect energy expenditure in humans.²⁵ While the FCC has been implicated within iWAT,²¹ the discrepancy between the present study and those previously reported from a single group identifying the presence of FCC may also relate to the tissue studied and method of assessing mitochondrial respiration. While originally

delineated in WAT/beige,²¹ FCC has been particularly emphasized in BAT.^{21,28,56} While it remains possible that FCC exists within BAT, the necessity of BAT for FCC is difficult to rectify with the observations that *SLC6A8* and *GATM* deletion impair WAT bioenergetics^{23,24} or the original finding that creatine stimulated *in vitro* respiration in iWAT following cold exposure. Alternatively, since creatine transport is sodium dependent, genetic models that affect creatine metabolism may indirectly influence energy expenditure through sodium-potassium ATPase activity (NaK-ATPase), as opposed to a direct stimulation of creatine kinase-mediated ADP recycling.

Another important consideration is the methodology used to interrogate mitochondrial bioenergetics, as previous work has exclusively utilized isolated mitochondria in UCP1 null/inhibited preparations.^{21,22} Key aspects of UCP1 biology remain to be identified, including the location of UCP1 on the inner mitochondrial membrane relative to other proteins influencing H⁺ availability (eg, ANT, ATP synthase, and complexes I, III, and IV), as well as how to model the biological flux through UCP1 with the “correct” concentration of metabolites (eg, purine nucleotides), pH, and morphology.^{48–51} As a result of these knowledge gaps, while we originally examined mitochondrial respiration in the presence of GDP-mediated inhibition of UCP1, we have primarily utilized a permeabilized tissue preparation without purposefully removing/inhibiting UCP1 function. While our permeabilized adipose tissue preparation maintains *in vivo* cellular structure, in contrast to isolated mitochondria, a caveat of a permeabilized preparation is that endogenous substrates may persist within the tissue, and while this may retain mitochondrial coupling/minimize UCP1 H⁺ conductance, it is conceivable that retained endogenous creatine concentrations already saturated the respiratory system, preventing the ability to further stimulate respiration with the provision of excessive exogenous creatine. However, this possible limitation does not extend to the *in vivo* observation that ablating *Ckmt1* does not influence whole-body responses to diverse metabolic stressors or that creatine exerts no stimulatory effects on respiration in isolated mitochondria. While CKB has been suggested to be important for cold-induced creatine-mediated ADP recycling, and CKB was identified in the proteome of human WAT, we could not detect changes in CKB following β_3 -adrenergic activation, challenging the contribution of this CK isoform to regulating energy expenditure within WAT. Additionally, while CKB has been proposed to stimulate respiration through the production of PCr and ADP, reductions in CKB appear to increase, not decrease, PCr concentrations, and stimulate respiration in human adipocytes,²⁹ suggesting CKB is not required for mitochondrial respiration. This finding is further suggested by a recent report not validating the presence of CKB on mitochondrial membranes.²⁹ Although we could not detect CKMT2 protein in human WAT, CKMT2 has previously been reported in the WAT of humans,²⁹ and is abundantly expressed in human WAT CD34⁺ progenitor cells (present study), suggesting this mitochondrial creatine kinase isoform may be biologically relevant to being/energy expenditure. Additionally, ANT-1 and ANT-2 are poorly expressed in CD34⁺ progenitor cells³⁹ creating the possibility of a greater reliance on creatine kinase-mediated ADP recycling to optimize ADP transport and mitochondrial oxidative phosphorylation. While CKMT2 has been detected on mitochondrial membranes within human WAT,²⁹ siRNA-mediated knockdown of CKMT2 only modestly affected mitochondrial creatine kinase activity,²⁹ suggesting this is not the only isoform on mitochondrial membranes within WAT. It is also unknown where CKMT1 and 2 are located on mitochondrial membranes, information that is required to further delineate the importance of these enzymes in the regulation of metabolism, as ANT-1 and ANT-2 reside in different locations⁶³ and recycling of ADP in close proximity to ANT isoforms may interact with OXPHOS proteins to functionally coordinate mitochondrial electron transport flux differently.⁶⁴ This information is particularly pertinent, as unlike in skeletal muscle ([ADP] < [creatine]),⁶⁵ within WAT total [ADP] is estimated to be greater than total [creatine],^{66,67} and while the concentrations of ADP/ATP and Cr/PCr within the intermembrane space, as well as the location of CK relative to ANT isoforms, remain

unknown within WAT, the relative abundance of ADP and Cr would not predict enzymatic flux towards the production of ADP (Cr+ATP \leftrightarrow PCr+ADP+H⁺). Together, these theoretical observations, in concert with the present data, indicate that creatine is unlikely to stimulate respiration within WAT.

In the present study, WAT/beige adipose tissue were examined because of the high abundance in obese individuals and potential to be exploited for therapeutic gain. A strength of the present study is the direct assessment of WAT mitochondrial respiration *ex vivo*; however, regardless of WAT/beige depot, creatine did not stimulate mitochondrial respiration in a variety of models. Additionally, despite our supposition that CKMT1 would be principally involved as a creatine kinase in the FCC, our data suggest that CKMT1 is not a primary contributor of this molecular pathway in beige adipose tissue (iWAT), at least in the context of pharmacological β_3 -AR stimulation and obesity. While it remains possible that FCC exists in BAT, the absence of a creatine-mediated response in WAT/beige (present data) and BAT following creatine supplementation,²⁵ and the increase in body weight associated with creatine supplementation^{68,69} challenges the therapeutic potential of modulating FCC to promote energy expenditure. Future work should nevertheless seek to clarify the proteins involved in creatine metabolism, and their biological significance within adipose tissue depots, particularly CKB and PCr, which have been linked to WAT inflammation²⁹ and sustained activation of the inflammasome.⁷⁰

Altogether, the present data provide evidence that (1) creatine does not drive mitochondrial respiration in differentiated beige adipocytes, isolated mitochondria or permeabilized adipose preparations, (2) despite the detection of *Ckmt1* in human adipocyte progenitor cells and CKMT1 protein in human WAT depots, (3) the expression of proposed FCC-related proteins were not coordinated in human WAT, (4) shRNA-mediated reductions in *Ckmt1* do not decrease mitochondrial respiration, and genetic ablation of *Ckmt1* in mice does not alter, (5) adrenergic-induced energy expenditure, (6) adipose tissue respiration, or (7) the biological responses to high-fat feeding. While creatine has been suggested to promote ADP-recycling, the present study suggests creatine and *Ckmt1* are not primary regulators of mitochondrial bioenergetics within WAT.

Supplementary material

Supplementary material is available at the APS Function online.

Supplemental Figure 1: The creatine-induced reduction of ADP sensitivity in permeabilized skeletal muscle fibers is impaired in *Ckmt1* KO mice. ADP respiratory kinetics with and without creatine (A) and with a rescaled x-axis of the Michaelis-Menten curve to highlight the kinetic shift (B) in WT and KO animals. Cr, creatine. Data expressed as mean \pm SEM.

Supplemental Figure 2: Quantified respiration in permeabilized white adipose tissue following 4 d of CL 316, 243 administration. PM, pyruvate + malate; G, glutamate; GDP, Cr, creatine. Data expressed as mean \pm SEM.

Supplemental Figure 3: *Ckmt1* KO mice exhibit comparable morphological changes in interscapular brown adipose tissue after 4 d of CL 316, 243 administration. Representative images of BAT stained with hematoxylin-and-eosin (H&E) from SAL and CL-treated mice imaged at x40 magnification from male *Ckmt1* WT and KO animals. Scale bars are 43 μ m.

Supplemental Figure 4: Whole-body responses to high-fat diet in male *Ckmt1* WT and KO mice. Glucose tolerance test (A),

area under the curve (B), VO_2 (C), VCO_2 (D), carbohydrate oxidation (E), lipid oxidation (F), RER (G), energy expenditure (H), and activity (I) in male *Ckmt1* WT and KO mice after 8 wk of LFD or HFD-feeding. Area under the curve; VO_2 , rate of oxygen consumption; VCO_2 , rate of carbon dioxide production; RER. Data expressed as mean \pm SEM.

Funding

This work was supported by the Natural Sciences and Engineering Research Council of Canada (NSERC) (grant number 400362 to G.P.H.). V.P.B., H.L.P., and G.J.D. were all funded by an NSERC graduate scholarship. Graphical abstract and figures with visual schematics were created with BioRender.com.

Author Contributions

V.P.B., H.L.P., A.R., G.J.D., H.B., and L.M.R. organized and performed experiments. V.P.B., D.C.W., and G.P.H. designed the study. All authors analyzed and interpreted the data. V.P.B. and G.P.H. drafted the manuscript, and all authors approved the final version.

Competing Interests

Drs. G.H. and M.W. are Editorial Board members for *Function* but were blinded from reviewing or making decisions regarding this manuscript.

Data Availability

The data sets generated during and/or analyzed during the current study are available from the corresponding author on reasonable request.

References

- Jacobsson A, Stadler U, Glotzer MA, et al. Mitochondrial uncoupling protein from mouse brown fat: molecular cloning, genetic mapping and mRNA expression. *J Biol Chem.* 1985;260(30):16250–16254.
- Hittelman KJ, Lindberg O, Cannon B. Oxidative phosphorylation and compartmentation of fatty acid metabolism in brown fat mitochondria. *Eur J Biochem.* 1969;11(1):183–192.
- Locke RM, Rial E, Scott ID, et al. Fatty acids as acute regulators of the proton conductance of hamster brown-fat mitochondria. *Eur J Biochem.* 1982;129(2):373–380.
- Lin CS, Klingenberg M. Isolation of the uncoupling protein from brown adipose tissue mitochondria. *FEBS Lett.* 1980;113(2):299–303.
- Nicholls DG. The bioenergetics of brown adipose tissue mitochondria. *FEBS Lett.* 1976;61(2):103–110.
- Klingenberg M, Winkler E. The reconstituted isolated uncoupling protein is a membrane potential driven H^+ translocator. *EMBO J.* 1985;4(12):3087–3092.
- Cypess AM, Lehman S, Williams G, et al. Identification and importance of brown adipose tissue in adult humans. *Obstet Gynecol Surv.* 2009;64(8):519–520.
- van Marken Lichtenbelt WD, Vanhommerig JW, Smulders NM, et al. Cold-activated brown adipose tissue in healthy men. *N Engl J Med.* 2009;360(15):1500–1508.
- Young P, Arch JRS, Ashwell M. Brown adipose tissue in the parametrial fat pad of the mouse. *FEBS Lett.* 1984;167(1):10–14.
- Cousin B, Cinti S, Morroni M, et al. Occurrence of brown adipocytes in rat white adipose tissue: Molecular and morphological characterization. *J Cell Sci.* 1992;103(4):931–942.
- Petrovic N, Walden TB, Shabalina IG, et al. Chronic peroxisome proliferator-activated receptor γ (PPAR γ) activation of epididymally derived white adipocyte cultures reveals a population of thermogenically competent, UCP1-containing adipocytes molecularly distinct from classic brown adipocytes. *J Biol Chem.* 2010;285(10):7153–7164.
- Danysz W, Han Y, Li F, et al. Browning of white adipose tissue induced by the β_3 agonist CL-316,243 after local and systemic treatment - PK-PD relationship. *Biochim Biophys Acta Mol Basis Dis.* 2018;1864(9):2972–2982.
- Wu J, Boström P, Sparks LM, et al. Beige adipocytes are a distinct type of thermogenic fat cell in mouse and human. *Cell.* 2012;150(2):366–376.
- Lshibashi J, Seale P. Beige can be slimming. *Science.* 2010;328(5982):1113–1114.
- Finlin BS, Memetimin H, Confides AL, et al. Human adipose beiging in response to cold and mirabegron. *JCI insight.* 2018;3(15):e121510.
- Shabalina IG, Petrovic N, deJong JMA, et al. UCP1 in Brite/Beige adipose tissue mitochondria is functionally thermogenic. *Cell Rep.* 2013;5(5):1196–1203.
- Sidossis LS, Porter C, Saraf MK, et al. Browning of subcutaneous white adipose tissue in humans after severe adrenergic stress. *Cell Metab.* 2015;22(2):219–227.
- Lee P, Werner CD, Kebebew E, et al. Functional thermogenic beige adipogenesis is inducible in human neck fat. *Int J Obes.* 2014;38(2):170–176.
- Min SY, Kady J, Nam M, et al. Human “brite/beige” adipocytes develop from capillary networks, and their implantation improves metabolic homeostasis in mice. *Nat Med.* 2016;22(3):312–318.
- Hausman DB, DiGirolamo M, Bartness TJ, et al. The biology of white adipocyte proliferation. *Obes Rev.* 2001;2(4):239–254.
- Kazak L, Chouchani ET, Jedrychowski MP, et al. A creatine-driven substrate cycle enhances energy expenditure and thermogenesis in beige fat. *Cell.* 2015;163(3):643–655.
- Bertholet AM, Kazak L, Chouchani ET, et al. Mitochondrial patch clamp of beige adipocytes reveals UCP1-positive and UCP1-negative cells both exhibiting futile creatine cycling. *Cell Metab.* 2017;25(4):811–822.e4.e4.
- Kazak L, Rahbani JF, Samborska B, et al. Ablation of adipocyte creatine transport impairs thermogenesis and causes diet-induced obesity. *Nat Metab.* 2019;1(3):360–370.
- Kazak L, Chouchani ET, Lu GZ, et al. Genetic depletion of adipocyte creatine metabolism inhibits diet-induced thermogenesis and drives obesity. *Cell Metab.* 2017;26(4):660–671.e3.
- Connell NJ, Doligkeit D, Andriessen C, et al. No evidence for brown adipose tissue activation after creatine supplementation in adult vegetarians. *Nat Metab.* 2021;3(1):107–117.
- Haas RC, Strauss AW. Separate nuclear genes encode sarcomere-specific and ubiquitous human mitochondrial creatine kinase isoenzymes. *J Biol Chem.* 1990;265(12):6921–6927.

27. Hossle JP, Schlegel J, Wegmann G, et al. Distinct tissue specific mitochondrial creatine kinases from chicken brain and striated muscle with a conserved CK framework. *Biochem Biophys Res Commun*. 1988;151(1):408–416.
28. Rahbani JF, Roesler A, Hussain MF, et al. Creatine kinase B controls futile creatine cycling in thermogenic fat. *Nature*. 2021;590(7846):480–485.
29. Maqdasy S, Lecoutre S, Renzi G, et al. Impaired phosphocreatine metabolism in white adipocytes promotes inflammation. *Nat Metabol*. 2022;4(2):190–202.
30. Müller S, Balaz M, Stefanicka P, et al. Proteomic analysis of human brown adipose tissue reveals utilization of coupled and uncoupled energy expenditure pathways. *Sci Rep*. 2016;6(30030).
31. Svensson PA, Jernås M, Sjöholm K, et al. Gene expression in human brown adipose tissue. *Int J Mol Med*. 2011;27(2):227–232.
32. Miotto PM, Holloway GP. In the absence of phosphate shuttling, exercise reveals the in vivo importance of creatine-independent mitochondrial ADP transport. *Biochem J*. 2016;473:18, 2831–2843.
33. Brunetta HS, Politis-Barber V, Petrick HL, et al. Nitrate attenuates high fat diet-induced glucose intolerance in association with reduced epididymal adipose tissue inflammation and mitochondrial reactive oxygen species emission. *J Physiol*. 2020;598(16):3357–3371.
34. Politis-Barber V, Brunetta HS, Paglialonga S, et al. Long-term, high-fat feeding exacerbates short-term increases in adipose mitochondrial reactive oxygen species, without impairing mitochondrial respiration. *Am J Physiol Endocrinol Metab*. 2020;319(2):E376–E387.
35. Beaudoin MS, Snook LA, Arkell AM, et al. Resveratrol supplementation improves white adipose tissue function in a depot-specific manner in Zucker diabetic fatty rats. *Am J Physiol Regul Integr Comp Physiol*. 2013;305(5):R542–R551.
36. Wan Z, Perry CGR, Macdonald T, et al. IL-6 is not necessary for the regulation of adipose tissue mitochondrial content. *PLoS One*. 2012;7(12):e51233.
37. Anderson EJ, Lustig ME, Boyle KE, et al. Mitochondrial H₂O₂ emission and cellular redox state link excess fat intake to insulin resistance in both rodents and humans. *J Clin Invest*. 2009;119(3):573–581.
38. Anderson EJ, Neuffer PD. Type II skeletal myofibers possess unique properties that potentiate mitochondrial H₂O₂ generation. *Am J Physiol Cell Physiol*. 2006;290(3):C844–C851.
39. Raajendiran A, Ooi G, Bayliss J, et al. Identification of metabolically distinct adipocyte progenitor cells in human adipose tissues. *Cell Rep*. 2019;27:1528–1540.
40. Raajendiran A, Krisp C, De Souza DP, et al. Proteome analysis of human adipocytes identifies depot-specific heterogeneity at metabolic control points. *Am J Physiol Metab*. 2021;320(6):E1068–E1084.
41. Rocha AL, de Lima TI, de Souza GP, et al. Enoxacin induces oxidative metabolism and mitigates obesity by regulating adipose tissue miRNA expression. *Sci Adv*. 2020;6:eabc6250
43. Peronnet F, Massicotte D. Table of nonprotein respiratory quotient : an update. *J Can des Sci du Sport*. 1991;16(1):23–29.
44. Smith BK, Perry CGR, Koves TR, et al. Identification of a novel malonyl-CoA IC50 for CPT-I: Implications for predicting in vivo fatty acid oxidation rates. *Biochem J*. 2012;448(1):13–20.
45. Holloway GP, Bezaire V, Heigenhauser GJF, et al. Mitochondrial long chain fatty acid oxidation, fatty acid translocase/CD36 content and carnitine palmitoyltransferase I activity in human skeletal muscle during aerobic exercise. *J Physiol*. 2006;571(1):201–210.
46. Martin BR, Denton RM. The intracellular localization of enzymes in white-adipose-tissue fat-cells and permeability properties of fat-cell mitochondria. Transfer of acetyl units and reducing power between mitochondria and cytoplasm. *Biochem J*. 1970;117(5):861–877.
47. Robinson BH, Halperin ML. Transport of reduced nicotinamide-adenine dinucleotide into mitochondria of rat white adipose tissue. *Biochem J*. 1970;116(2):229–233.
48. Nicholls DG, Rial EA. A history of the first uncoupling protein, UCP1. *J Bioenerg Biomembr*. 1999;31(5):399–406.
49. Picard M, Taivassalo T, Ritchie D, et al. Mitochondrial structure and function are disrupted by standard isolation methods. *PLoS One*. 2011;6(3):1–12.
50. Barkhade T, Mahapatra SK, Banerjee I. Study of mitochondrial swelling, membrane fluidity and ROS production induced by nano-TiO₂ and prevented by Fe incorporation. *Toxicol Res*. 2019;8(5):711–722.
51. Nath S. Molecular mechanistic insights into uncoupling of ion transport from ATP synthesis. *Biophys Chem*. 2018;242:15–21.
52. Steeghs K, Heerschap A, De Haan A, et al. Use of gene targeting for compromising energy homeostasis in neuromuscular tissues: The role of sarcomeric mitochondrial creatine kinase. *J Neurosci Methods*. 1997;71(1):29–41.
53. Ingvorsen C, Karp NA, Lelliott CJ. The role of sex and body weight on the metabolic effects of high-fat diet in C57BL/6N mice. *Nutr Diabetes*. 2017;7(4):e261–7.
54. Medrikova D, Jilkova ZM, Bardova K, et al. Sex differences during the course of diet-induced obesity in mice: Adipose tissue expandability and glycemic control. *Int J Obes*. 2012;36(2):262–272.
55. Feldmann HM, Golozoubova V, Cannon B, et al. UCP1 ablation induces obesity and abolishes diet-induced thermogenesis in mice exempt from thermal stress by living at thermoneutrality. *Cell Metab*. 2009;9(2):203–209.
56. Sun Y, Rahbani JF, Jedrychowski MP, et al. Mitochondrial TNAP controls thermogenesis by hydrolysis of phosphocreatine. *Nature*. 2021;593(7860):580–585.
57. Jiang Y, Berry DC, Graff JM. Distinct cellular and molecular mechanisms for β 3 adrenergic receptor-induced beige adipocyte formation. *Elife*. 2017;6:e30329.
58. de Jong JMA, Wouters RTF, Boulet N, et al. The β 3-adrenergic receptor is dispensable for browning of adipose tissues. *Am J Physiol Endocrinol Metab*. 2017;312(6):E508–E518.
59. Kazak L, Rahbani J, Scholtes C, et al. Combined α - and β -adrenergic receptor activation triggers thermogenesis by the futile creatine cycle. *Res Sq*. 2022, 10.21203/rs.3.rs-1190032/v1 PPR443405.
60. Zhao J, Unelius L, Bengtsson T, et al. Coexisting β -adrenoceptor subtypes: significance for thermogenic process in brown fat cells. *Am J Physiol Cell Physiol*. 1994;267(4):C969–C979.
61. Zhao JIN, Cannon B, Nedergaard JAN, Cannon B, Nedergaard J. Thermogenesis is β 3- but not β 1-adrenergically mediated in rat brown fat cells, even after cold acclimation. *Am J Physiol Regul Integr Comp Physiol*. 1998;275(6):R2002–R2011.
62. Gonçalves LF, Machado TQ, Castro-Pinheiro C, de Souza NG, Oliveira KJ, Fernandes-Santos C. Ageing is associated with brown adipose tissue remodelling and loss of white fat browning in female C57BL/6 mice. *Int J Exp Pathol*. 2017;98(2):100–108.

63. Vyssokikh MY, Katz A, Rueck A., et al. Adenine nucleotide translocator isoforms 1 and 2 are differently distributed in the mitochondrial inner membrane and have distinct affinities to cyclophilin D. *Biochem J.* 2001;**358**(2):349–358.
64. Lu YW, Acoba MG, Selvaraju K., et al. Human adenine nucleotide translocases physically and functionally interact with respirasomes. *Mol Biol Cell.* 2017;**28**(11):1489–1506.
65. Kushmerick MJ, Moerland TS, Wiseman RW. Mammalian skeletal muscle fibers distinguished by contents of phosphocreatine, ATP, and Pi. *Proc Natl Acad Sci* 1992;**89**(16):7521–7525.
66. Denton RM, Yorke RE, Randle PJ. Measurement of concentrations of metabolites in adipose tissue and effects of insulin, alloxan-diabetes and adrenaline. *Biochem J.* 1966;**100**(2):407–419.
67. Berlet HH, Bonsmann I, Birringer H. Occurrence of free creatine, phosphocreatine and creatine phosphokinase in adipose tissue. *Biochim Biophys Acta Gen Subj.* 1976;**437**(1):166–174.
68. Balsom PD, Ekblom B, Söerlund K., et al. Creatine supplementation and dynamic high-intensity intermittent exercise. *Scand J Med Sci Sports.* 1993;**3**(3):143–149.
69. Stroud MA, Holliman D, Bell D., et al. Effect of oral creatine supplementation on respiratory gas exchange and blood lactate accumulation during steady-state incremental treadmill exercise and recovery in man. *Clin Sci (Colch).* 1994;**87**(6):707–710.
70. Billingham LK, Stoolman JS, Vasan K., et al. Mitochondrial electron transport chain is necessary for NLRP3 inflammasome activation. *Nat Immunol.* 2022;**23**: 692–704.